Pis'ma v ZhETF, vol. 96, iss. 2, pp. 135 – 138

Metallic layer inside the Earth's lower mantle

S. G. Ovchinnikov[+*1)], T. M. Ovchinnikova[×], P. G. Dyad'kov[°], V. V. Plotkin[°], K. D. Litasov[▽]

[+] Kirensky Institute of Physics SB RAS, 660036 Krasnoyarsk, Russia

[*] Siberian Federal University, 660041 Krasnoyarsk, Russia

[×] Sukhachev Institute of Forest SB RAS, 660036 Krasnoyarsk, Russia

[°] Trofimuk Institute of Petrolium-Gas Geology and Geophysics SB RAS, 630090 Novosibirsk, Russia

[▽] Sobolev Institute of Geology and Mineralogy SB RAS, 630090 Novosibirsk, Russia

Submitted 12 April 2012

Resubmitted 13 June 2012

We predict the insulator-metal-insulator transitions for the temperature and pressure of the lower mantle with the metal layer thickness $\Delta h \approx 400$ km at the depth of 1400–1800 km. The insulator-metal transition has the Mott–Hubbard origin, while the second transition from metal to insulator results from spin crossover of the Fe^{2+} ions from high spin $S = 2$ to low spin $S = 0$ state. The conductivity in the metal layer may attain 250 S/m. The depth profile of the conductivity is also suggested.

The lower mantle extends from 660 to 2900 km with pressure increase from 24 to 135 GPa and temperature increase from 2070 to 2750 K [1–4]. The electrical conductivity is one of the important physical properties of the Earth's mantle. The lower mantle consists of 79% Mg-perovskite $Mg_{0.9}Fe_{0.1}SiO_3$, 16% magnesiowustite $Mg_{1-x}Fe_xO$ ($x = 0.15 \sim 0.20$), and 5% $CaSiO_3$ perovskite in volume, and the electrical conductivity occurs through iron-bearing phases. At normal conditions all of them are insulators. At pressures of the lower mantle the insulator-metal transition can be expected [5].

The possible existence of the highly conductive layer has been suggested in the mantle from geophysical modeling [6, 7]. The MAGSAT vector measurements have been inverted in terms of conductivity that results in increase of conductivity in the upper parts of the lower mantle, with a jump to 200 S/m at the depth of 1300 km [8]. The laboratory measurements of the Mg-perovskite conductivity at pressures up to 143 GPa have demonstrated conductivity increase in the post-perovskite phase [9] without metallization up to the highest pressure. Similar measurements of the magnesiowustite in a diamond-anvil cell at room temperature and pressures up to 135 GPa have revealed a maximum in pressure dependence of the conductivity $\sigma(P)$ near $P \approx 60$ GPa for the composition $Mg_{0.81}Fe_{0.19}O$ [10] and $Mg_{0.75}Fe_{0.25}O$ [11]. This maximum was related to the spin crossover from the high spin to the low spin state of the Fe^{2+} ion. This spin crossover has been found between 60 and 70 GPa by measuring the X-ray emission spectra [12] and the Mössbauer spectra [13] at room temperature.

Magnesiowustite is a solid solution between periclase MgO, a wide band gap insulator, and wustite FeO, a classical Mott-Hubbard insulator among the strongly correlated transition metal monoxide group [5, 14]. Theoretical analysis of the pressure dependent electronic structure of the magnesiowustite within the multielectron LDA+GTB approach [15] with account for strong electron correlations results in the PT-phase diagram [16] where both the Mott–Hubbard metallization and spin crossover take place. Compare this phase diagram with the depth profile for the pressure and temperature in the lower mantle we can determine magnesiowustite phase diagram as a function of depth (Fig. 1). The pressure dependence of the electronic structure results in the closure of the Mott–Hubbard d–d band gap at the critical value P_M and in the crossover of the high and low spin energy levels for the Fe^{2+} ion at the critical value P_S (for zero temperature). The band structure calculations for FeO by the LDA+DMFT method taking into account strong electron correlations lead to the prediction of the Mott–Hubbard transition at $P_M = 60$ GPa [17]. In a large number of iron oxides the value P_S falls in the same pressure range 50–70 GPa [18]. Recently, the low temperature ($T = 5$ K) synchrotron Mössbauer spectroscopy of the magnesiowustite $Mg_{0.75}Fe_{0.25}O$ has revealed a very narrow region of spin fluctuations with the critical point at $P_S = 56$ GPa [19]. Within the experimental uncertainty of the pressure measurement $P_S = P_M$, and we have assumed that at $T = 0$ both

[1)] e-mail: sgo@iph.krasn.ru

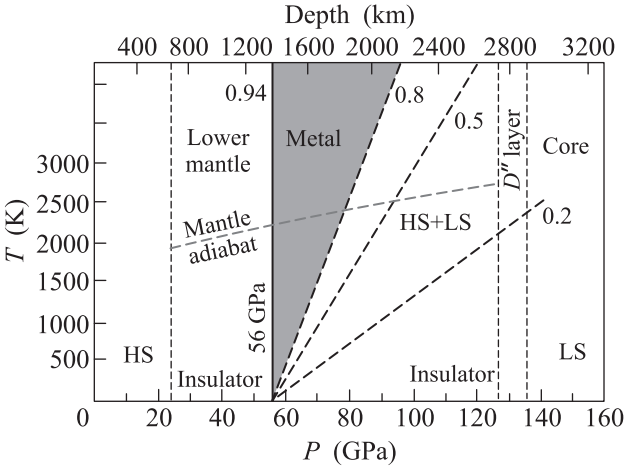

Fig. 1. Magnesiowustite phase diagram. Bold dashed line indicates temperature and pressure profiles in lower mantle. The vertical dash-dotted lines show the lower mantle border, the $D^{||}$ layer and the outer core border. At zero temperature there is the critical point PC that separates high spin (HS) and low spin (LS) states, as well as insulator and metal. Numbers at the straight lines starting from the critical point show the concentration of high spin states

metallization and spin crossover occur at a single critical point P_c.

We should clarify why the insulator-metal transition in FeO is relevant to the $Mg_{1-x}Fe_xO$ properties. According to the percolation theory a random mixture of the insulator MgO and metal FeO will conduct the electric current if the concentration x is above the percolation threshold x_c. For fcc crystal lattice $x_c = 0.142$ [20]. For the same reason a mixture of insulator Mg-perovskite and metallic magnesiowustite will also have metallic conductivity. The data for Fe^{2+}-disproportionation into Fe^{3+} in Mg-perovskite and Fe^0 indicate that the lower mantle may contain 1–2% of Fe-metal [21]. Since percolation threshold is determined by the total metallic volume, the Fe-metal impurity decreases a critical concentration of metallic ferropericlase required for metallization of the lower mantle by 1–2 wt%.

The activation energy E_a of the Mott–Hubbard insulator may be estimated as follows [5]

$$E_a = (U_{\text{eff}} - W)/2, \tag{1}$$

where W is the half bandwidth increasing with pressure due to decreasing interatomic distance. The effective Coulomb parameter U_{eff} for the d^6 electron configuration is equal to

$$U_{\text{eff}}(d^6) = E_0(d^7) + E_0(d^5) - 2E_0(d^6), \tag{2}$$

where $E_0(d^n)$ is the lowest energy term for the d^n-configuration. At ambient pressure Fe^{2+} has the high spin ground term with U_{eff}(HS)=A-5B. Here A, B, and C (below) are the Raccah parameters (Coulomb interaction). Due to crystal field parameter 10Dq growth with pressure the low spin state becomes the ground term at $P > P_S$. It results in the U_{eff} increase [22], U_{eff}(LS)=A+4B-2C+10Dq. This increase of the U_{eff} in the low spin state is the reason why the metallization in the high spin state may be accompanied by the reentrant transition into insulator state with further pressure increase.

At finite temperature the spin-crossover is not a thermodynamic phase transition. Each Fe^{2+} ion may be in the high spin state with the probability n_{HS} and in the low spin state with $n_{\text{LS}} = 1 - n_{\text{HS}}$. The fixed n_{HS} lines in the Fig. 1 are given by

$$P = P_c + kT \ln \frac{g_{\text{HS}} n_{\text{LS}}}{g_{\text{LS}} n_{\text{HS}}} \Big/ 2\frac{\partial(10Dq)}{\partial P}, \tag{3}$$

where g_{HS} (g_{LS}) are the degeneracy degree of the high (low) spin state. For Fe^{2+} ion in the low spin state with spin $S = 0$ and orbital moment $L = 0$ $g_{\text{LS}} = (2S+1)(2L+1) = 1$. In the high spin state with $S = 2$ and $L = 1$ $g_{\text{HS}} = 15$. If both g_{HS} and g_{LS} were equal the maximal spin fluctuations line $n_{\text{HS}} = n_{\text{LS}}$ would be the vertical line from the P_C in the Fig. 1. Due to large difference in the degeneracy the line $n_{\text{HS}} = n_{\text{LS}} = 0.5$ is significantly inclined to the right in the Fig. 1. It means that the pressure corresponding to the "smoothed spin crossover" at finite T increases linearly with T (see the Eq. (3)).

The pressure dependence of the activation energy is shown in the Fig. 2a. The model parameters have been chosen to reproduce the activation energy $E_a \approx 0.3$ eV at ambient pressure [23], and $E_a = 0.27$ eV at 101 GPa [11]. The linear decrease of the activation energy at small pressure corresponds to the negative activation volume of the conductivity analysis from the chemical point of view [4]. The negative E_a at $56 < P < 77$ GPa indicates the metal state. The sharp increase of the activation energy results from U_{eff} growth in the low spin state. We can estimate the conductivity as

$$\sigma(P,T) = \sigma_0 \exp[-E_a(P,T)/kT]. \tag{4}$$

To find the σ_0 value we use the experimental data [4, 23]: for $x = 0.194$, $T = 1000$ K, $P = 5$ GPa, and $\sigma = 10$ S/m. With our activation energy 0.27 eV from the Fig. 2 we estimate $\sigma_0 \approx 230$ S/m.

The depth profile of conductivity is shown in the Fig. 2b. At the upper border between insulator and

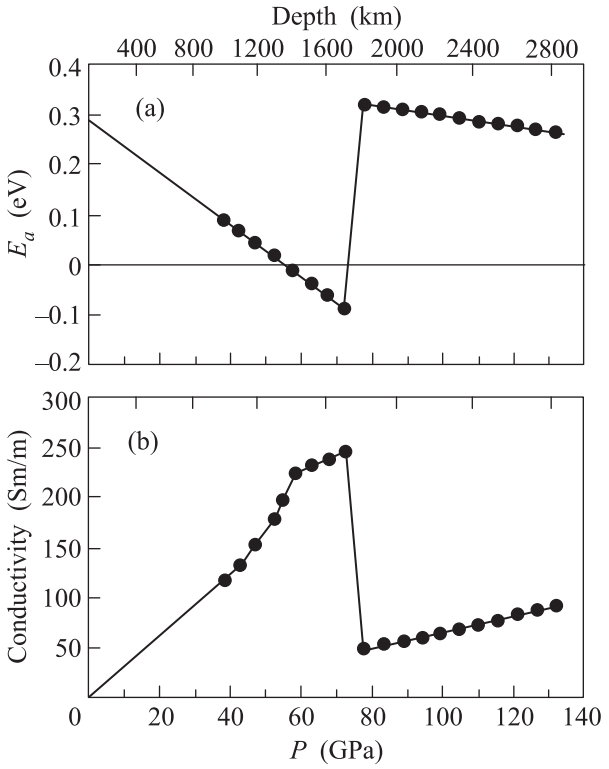

Fig. 2. Pressure dependence of the activation energy (a) and the depth profile of conductivity (b). The decrease at small pressure with closure of the gap at 56 GPa is due to the Mott–Hubbard transition. The reentrant metal-insulator transition at 77 GPa results from the spin crossover. Negative Ea interval of pressure corresponds to the metal region in the Fig. 1 along the bold dash line

metal the change of conductivity is smooth due to high temperature and small insulator gap close to the Mott–Hubbard transition. Nevertheless metal state has positive derivative of the resistivity by temperature and thus differs from insulator where the same derivative is negative. In the metal region we take into account the additional growth of the conductivity of free electrons $\sigma \sim k_F^2 \sim V^{-2/3}$, where k_F is the Fermi wavenumber and V is the volume. The change of conductivity at the lower border is sharp due to the large jump of the gap induced by spin crossover.

We should emphasize that calculation of the conductivity with the Eq. (3) may be considered only as a qualitative estimation. Nevertheless our prediction of the metal layer inside the insulator lower mantle has general character. The maximal value of conductivity in the metal layer is about 250 S/m. Recently the experimental and theoretical evidence for pressure-induced metallization in FeO at pressures above 70 GPa and temperatures of 1900 K has been demonstrated [24] by measuring resistivity in the laser-heated diamond anvil cell. This work also confirms the first conclusion on the existence of a high-pressure metallic phase of FeO obtained under shock loading [25]. As we have discussed above the metallic FeO will result in the metallic magnesiowustite $Mg_{1-x}Fe_xO$ for x above the percolation threshold. Nevertheless the phase diagram of FeO and $Mg_{1-x}Fe_xO$ cannot be identical in spite of the similar crystal structure. The ionic radii of the Mg^{2+} is 0.072 nm while for the Fe^{2+} it is larger (0.078 nm). It means that the Fe^{2+} ion embedded into the MgO lattice is in the crystal field with smaller cation-anion distance than in FeO. This difference in the ionic radii induced additional chemical pressure in the magnesiowustite relative to FeO. The other difference of the FeO and magnesiowustite electronic structure is more narrow bands in magnesiowustite due to the large Fe–Fe interatomic distance. Thus we can compare the FeO and $Mg_{1-x}Fe_xO$ phase diagrams only qualitatively. Our calculations predict metallic $Mg_{1-x}Fe_xO$ at high temperature and pressure, which is consistent with experimental data [24]. Moreover, at low temperatures the theoretical calculations [24] also predict a narrow pressure range, where the FeO is in high-spin metallic state at pressures near 70 GPa, but it becomes a low spin insulator at higher pressures. We came to the similar conclusion for magnesiowustite. The measured and calculated value for FeO conductivity was about 10^4 S/m [20]. Our values for magnesiowustite are much lower because at the percolation threshold the conductivity tends to zero, and $Mg_{1-x}Fe_xO$ with $x = 0.16–0.20$ is close to the threshold. Our estimation for conductivity and its sharp increase at the depth of 1400 km agrees well with the paper [8].

In summary, we predict existence of a conductive metallic layer governed by metallization of magnesiowustite at approximately 1400–1800 km depth inside the lower mantle (Fig. 3). This theoretical conclusion should be verified by the laboratory measurements of

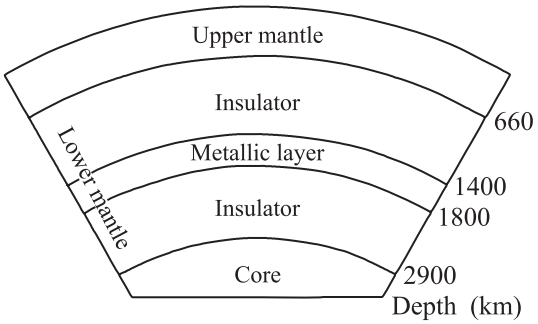

Fig. 3. The Earth's interior structure with predicted metallic layer in the lower mantle

the magnesiowustite resistivity at pressures 40–80 GPa and temperatures 2000–2500 K.

We are thankful to Dr.V.I. Anisimov for the discussions. This work was supported by Presidium of RAS project # 2.16, Siberian Branch of RAS project # 96 and 97, and by RFBR Grant # 12-02-90410.

1. N. L. Dobretsov, A. G. Kirdyashkin, and A. A. Kirdyashkin, *Glubinnaya geodinamika*, Novosibirsk: SORAN, filial "GEO", 2001.
2. F. D. Stacey and P. M. Davis, *Physics of the Earth*, 4th edition, Cambridge University Press, Cambridge, UK, 2008, 532 p.
3. Yu. M. Pusharovskii and D. Yu. Pusharovskii, *Geologiya mantii Zemli*, Moscow: GEOS, 2010.
4. Y. Xu, T. J. Shankland, and B. T. Poe, J. Geophys. Res. **105**, 27865 (2000).
5. N. F. Mott, *Metal-insulator transitions*, Taylor and Francis LTD, London, 1974.
6. L. N. Porokhova, D. Yu. Abramova, and D. A. Potokhov, Earth Planets Space **51**, 1067 (1999).
7. B. A. Buffett, E. J. Garnero, and R. Jeanloz, Science **290**, 1338 (2000).
8. S. Constable and C. Constable, Geochem. Geophys. Geosyst. **5**, 3 (2004).
9. K. Ohta, S. Onoda, K. Hirose et al., Science **320**, 89 (2008).
10. K. Ohta, K. Hirose, S. Onoda, and K. Shimizu, Proc. Jpn. Acad. B **83**, 97 (2007).
11. J. F. Lin, S. T. Weir, D. D. Jackson et al., Geophysical Research Lett. **34**, L16305 (2007).
12. J. Badro et al., Science **300**, 789 (2003).
13. I. S. Lyubutin et al., JETP Lett. **90**, 617 (2009).
14. R. E. Cohen, I. I. Mazin, and D. G. Isaak, Science **275**, 654657 (1997).
15. S. G. Ovchinnikov et al., *LDA+GTB Method for Band Structure Calculations in the Strongly Correlated Materials*, in: *Strongly Correlated Systems. Theoretical Methods* (ed. by A. Avella and F. Mancini), Springer Series is Solid State Sciences, Springer-Verlag, 2012, № 171, p. 143.
16. S. G. Ovchinnikov, JETP Lett. **94**, 192 (2011).
17. A. O. Shorikov et al., Phys. Rev. B **82**, 195101 (2010).
18. I. S. Lyubutin and A. G. Gavrilyuk, Phys. Usp. **52**, 989 (2009).
19. I. S. Lyubutin et al., *Quantum Critical Point and Spin Fluctuations in the Lower-mantle Ferropericlase*, Arxiv 1110.3956.
20. J. M. Ziman, *Models of Disorder*, Cambridge Univ. Press, 1979.
21. D. J. Frost et al., Nature **428**, 409 (2004).
22. S. G. Ovchinnikov, JETP **107**, 140 (2008).
23. D. P. Dobson, N. C. Richmond, and J. P. Brodholt, Science **275**, 1779 (1997).
24. K. Ohta et al., Phys. Rev. Lett. **108**, 026403 (2012).
25. E. Knittle and R. Jeanloz, Geophys. Res. Lett. **13**, 1541 (1986).